J Solid State Electrochem (2009) 13:1251–1257
DOI 10.1007/s10008-008-0658-4

ORIGINAL PAPER

Nickel oxide coated on ultrasonically pretreated carbon nanotubes for supercapacitor

Bo Gao · Chang-zhou Yuan · Lin-hao Su · Li Chen · Xiao-gang Zhang

Received: 13 May 2008 / Revised: 7 July 2008 / Accepted: 19 August 2008 / Published online: 5 September 2008

Abstract Nickel oxide/carbon nanotubes (NiO/CNTs) composite materials for supercapacitor are prepared by chemically depositing nickel hydroxide onto carbon nanotubes pretreated by ultrasonication and followed by thermal annealing at 300 °C. A series of NiO/CNTs composites with different weight ratios of nickel oxide versus carbon nanotubes are synthesized via the same route. The high-resolution TEM and SEM results show that a lot of nicks, which favored the nucleation of the nickel hydroxide formed on the outer walls of carbon nanotubes due to ultrasonic cavitations, and then nickel oxide coated uniformly on the outer surface of the individual carbon nanotubes. The NiO/CNTs electrode presents a maximum specific capacitance of 523 F/g as well as a good cycle life during 1,000 cycles in 6 M KOH electrolyte. The good electrochemical characteristics of NiO/CNTs composite can be attributed to the three-dimensionally interconnected nanotubular structure with a thin film of electroactive materials.

Keywords Carbon nanotubes · Nickel oxide · Supercapacitor · Ultrasonic cavitations

Introduction

Electrochemical capacitors (ECs), combining the advantages of the high power of dielectric capacitors and the high specific energy of rechargeable batteries, have played an increasingly important role in power source applications such as digital communications, hybrid electric vehicles, short-term power sources for mobile electronic devices. In these ECs, charge storage arises from either the nonfaradaic capacitive process based on charge separation at the electrode/solution interface, or the pseudocapacitive process containing faradaic redox reactions, which occur within the active electrode materials [1]. The most widely used active electrode materials for ECs are normally carbon with a high surface area [2], conducting polymers [3, 4] and transition metal oxides [5–19]. An amorphous phase of $RuO_2 \cdot xH_2O$ formed by the sol–gel method at low temperatures exhibits outstanding properties (e.g., high specific capacitance of 768 F/g and excellent cycle life in an acidic electrolyte) among many transition metal oxide materials investigated as a pseudocapacitor material [5]. However, the high cost and scarce source of ruthenium material limit its commercial applications. Therefore, some other electrochemical materials such as nickel oxide [6], cobalt oxide [16], manganese oxide [17–19], Ti–V–W oxides [20] and nitrides [21] of V, Nb, Mo, and W have been study widely due to their inexpensive characteristic, high theoretical capacity and pseudocapacitive behavior similar to that of hydrous RuO_2.

Nickel oxide (NiO) is being considered as one of promising potential electrode material for ECs as well as for many other applications such as catalyst, electrochromic films, fuel cell electrodes and gas sensors. It can be prepared by several methods (e.g., sol–gel method and liquid-phase process [13]) and the specific capacitances of these NiO materials were about 200–300 F/g. However, the specific capacitance of NiO reported previously is still far from its theoretical value (2,584 F/g within 0.5 V), indicating the low utilization of NiO materials. Furthermore, NiO has a high resistivity, which is another drawback

B. Gao · C.-z. Yuan · L.-h. Su · L. Chen · X.-g. Zhang (✉)
College of Material Science and Engineering,
Nanjing University of Aeronautics and Astronautics,
Nanjing 210016, People's Republic of China
e-mail: azhangxg@163.com

for practical applications to ECs. So it is crucial to enhance the capability and conductivity of NiO material in order to improve the energy density and power density.

It is well-known that the specific capacitance is directly related to the specific surface area of electrodes contact with electrolyte. And many work from our group show that the utilization of capacitive active materials can be improved by coating them on some substrates with high specific surface area [22–24]. Therefore, carbon nanotubes (CNTs), owing to their chemical stability, good conductivity, and large surface area, are thereby being considered as attractive substrates for ECs. Recently, Nam et al. [25] reported a nickel oxide/carbon nanotube ($Ni_{1-x}O$/CNT) film nanocomposite prepared by electrochemically precipitation. The specific capacitance of the composite electrode was exceeding 1,000 F/g, many times than that prepared by the conventional method, indicating great prospects of application of CNTs in supercapacitor materials. However, due to the intact and smooth surface of CNTs as well as poor solubility in solvents originated from van der Waals attractions, loading electrochemical materials on surface of CNTs via conventional methods was rather difficult. Therefore, many efforts have been focused on the functionalization of CNTs [26–34]. But to the best of our knowledge, the functionalization was often confined to the chemical methods, which are normally complicated and time-consuming.

In this paper, a physical ultrasonication method is employed to functionalize CNTs as carbonaceous substrate to form NiO/CNTs composite materials for ECs. The high-resolution TEM (HRTEM) and SEM results show that a lot of nicks are formed on the outer walls of carbon nanotubes due to ultrasonic cavitations, which favored the nucleation of the nickel hydroxide, and that nickel oxide is coated uniformly on the outer surface of the individual carbon nanotubes. Electrochemical tests demonstrate that the electrochemical performances of NiO/CNTs composites are improved greatly. The NiO/CNTs composite gives a maximum specific capacitance of 523 F/g and good cycle life, which can attribute to the three-dimensionally interconnected nanotubular structure with a thin film of electroactive materials.

Experimental

Purification of CNTs

Multi-walled carbon nanotubes (MWCNTs) were purchased from Shenzhen Nanotech Port Co. (China). The pristine CNTs are refluxed in 68 wt. % HNO_3 for 24 h at 40 °C to remove the catalyst impurities, and washed by deionized water and ethanol, then allowed to dry for 24 h under vacuum at 50 °C.

Synthesis of NiO/CNTs composites

The NiO/CNTs composites are prepared by a chemical precipitation followed by thermal annealing. Briefly, the CNTs are pretreated by ultrasonication for 5 h in 200 ml ethanol solution, then the nickel chloride hexahydrate ($NiCl_2$•$6H_2O$) powder is added to get 0.01 M solution of nickel chloride in CNTs suspension. Aqueous solution of NaOH of 0.01 M is added dropwise to the mixed aqueous solution containing CNTs and $NiCl_2$ with vigorous magnetic stirring until a dark precipitation of $Ni(OH)_2$/CNTs composite is formed. The precipitate is filtered using a centrifugal filtration method and washed with deionized water and ethanol, followed dried under vacuum for 24 h at 50 °C. Finally, the $Ni(OH)_2$/CNTs composites are calcined at 300 °C for 2 h to obtain the final product NiO/CNTs. A series of NiO/CNTs composites with mass ratio of NiO versus CNTs 4:6, 5:5, 6:4, 7:3, and 8:2 are synthesized by same route.

Measurement of structure and morphology

The structure and morphology properties of NiO/CNTs composites are characterized by several techniques. The structural characterization is performed by XRD (X-ray powder diffraction) (Mac M18ce, Japan) (diffractometer with Cu Kα radiation and λ=1.54056 Å in 2θ=10~80°). SEM (Scanning Electron Microscope) (LEO1430VP, Germany), TEM (Transmission Electron Microscope) (Hitachi-600, Japan) and high-resolution transmission electron microscopy (HRTEM) (JEM-3000, Japan) are used to observe the morphology of active materials.

Measurement of electrochemical properties

Electrodes for supercapacitors are prepared by mixing the active material with 25 wt% carbon (acetylene black) and 5 wt% PTFE (polytetrafluoroethylene). This mixture then mixed with a small amount of deionized water to make a homogeneous mixture, and is pressed on treated nickel grid (1.2×10^7 Pa). All electrochemical measurements are done by a three-electrode system equipped with the working electrode (sample electrode), a platinum foil counter electrode, and a standard calomel reference electrode (SCE). Electrochemical performance is investigated by cyclic voltammetry using CHI660 electrochemical workstation (Shanghai, China) with different voltage scan rates. For charge/discharge test of the active materials, an Arbin battery tester BT2000 is used. The experiments are carried out with 2–20 mA/cm^2 current density in the range of −0.1 to 0.4 V. All measurements are carried out in 6 M KOH electrolyte solution.

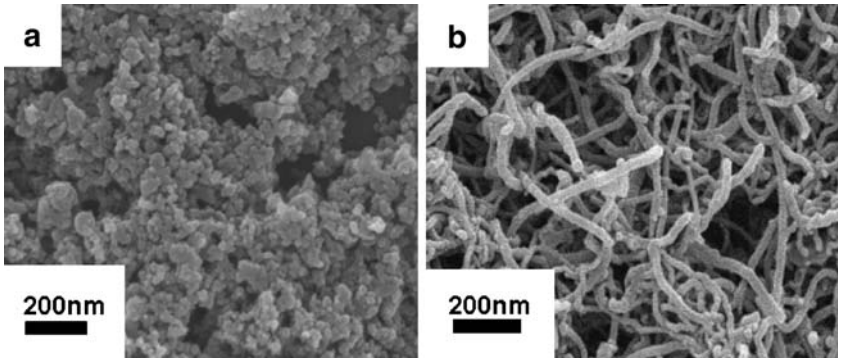

Fig. 1 SEM images of pure NiO (**a**) and CNTs (**b**)

Results and discussion

Characterization of the microstructure

Figure 1a shows the SEM image of pure NiO powder. The primary NiO powder consists of small particles, and a few primary particles aggregate into large secondary particles. Figure 1b shows typical SEM image of the multi-walled CNTs. The CNTs are a few micrometers in length. The diameters are widely distributed in pristine sample from smaller ones of 30–40 nm to larger ones of 60–70 nm. Furthermore, the CNTs are randomly entangled and cross-linked.

Figure 2 shows the SEM images of NiO/CNTs composites with different mass ratios of NiO versus CNTs (Fig. 2a: 8:2; Fig. 2b: 5:5). As shown in Fig. 2a, nanotubular material and a mass of particulate NiO are observed, which may be attribute to deficient surface and active sites provide by CNTs for NiO coating in such kind of NiO/CNTs. Hence there is a part of NiO still exists as grain form. In contrast with Fig. 2a, the NiO particles are not observed any longer in Fig. 2b and active composites are almost nanotubular shape when the ratio of CNTs increases. Therefore, the most important factor affecting the coating of NiO is the mass ratio of CNTs versus NiO.

Figure 3 shows the HRTEM images of CNTs (after the sonication process) and NiO/CNTs composite with the mass ratio of NiO/CNTs=5:5. In Fig. 3a, it is obvious that plenty of nicks are observed on the outer surface of CNTs, which caused by ultrasonic cavitations. Ultrasonic cavitations cause a very highly localized high temperature and pressure (>5000 K, >100 MPa) region on the outer surface of CNTs where tiny bubbles are collapsing—a region referred to as a "hot spot" [35–37]. In an ultrasonic cavitations field, these "hot spot" with extremely very high temperature and pressure, would destroy the outer wall of carbon nanotubes and form so-called "nick". The resulting nicks can act as nucleation sites to favor the Ni $(OH)_2$ nucleating and to coat NiO on CNTs [9, 38]. In Fig. 3b, it is clear that the NiO is coated uniformly on the outer surface of CNTs with a central hollow tube. The coating thickness is approximately 4–5 nm. Such structure will improve capacitive performance of NiO because the better electrochemical behavior was always associated with the high surface area.

The powder XRD patterns of the samples prepared in our experiment are shown in Fig. 4. In comparison, the pure NiO and CNTs are also listed in it. As shown in Fig. 4, the XRD patterns of different ratio of NiO/CNTs composites are the superposition of that of NiO and CNTs. The XRD

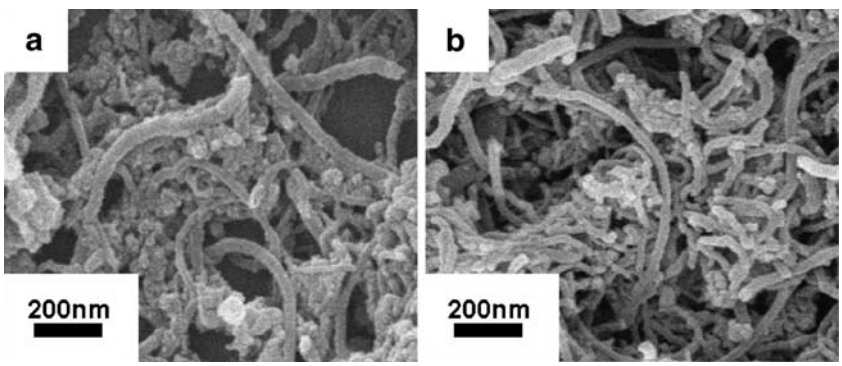

Fig. 2 SEM images of NiO/CNTs: (**a**) NiO/CNTs=8:2 and (**b**) NiO/CNTs=5:5

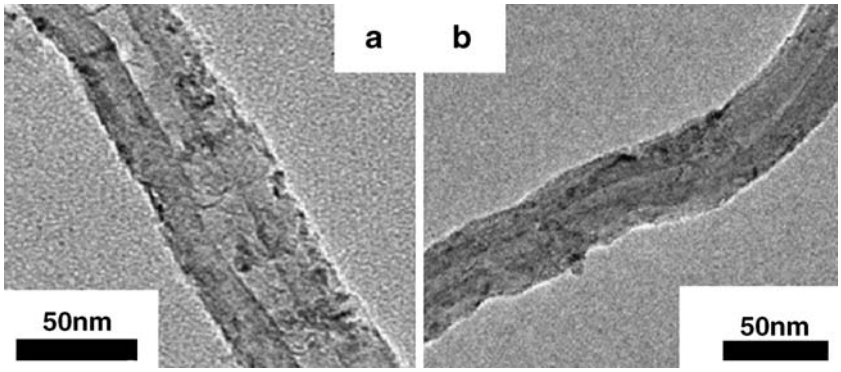

Fig. 3 High-resolution TEM images of CNTs after ultrasonication (**a**) and NiO/CNTs with mass ratio of NiO/CNTs=5:5 (**b**)

patterns of pure NiO and NiO/CNTs clearly exhibit typical diffraction peaks of NiO at 2θ=37.3°, 43.3°, and 62.9° (corresponding to (111), (200), and (220) reflections, respectively), which accords with a rhombohedral crystalline structure NiO (JCPDS Card No. 44–1159). The CNTs peak is also seen near 26° in different ratio of NiO/CNTs composites, which is referred to graphite (002) plate of multi-walled CNTs [39]. Moreover, the intensity of (002) reflections of CNTs in different composites decreased, compared with that of pure CNTs, indicating the coating of NiO on CNTs. The results above (SEM, HRTEM and XRD) have obviously proved that NiO is successfully coated on the outer surface of CNTs.

Electrochemical characterization

Cyclic voltammetry (CV) is employed to determine the electrochemical properties of the NiO/CNTs electrodes in 6 M KOH. Figure 5 shows the CV curves of the NiO/CNTs with different mass ratios and pure NiO electrodes at scan rates of 10 mV/s. The electrode potential is scanned between −0.1 and 0.4 V (vs. SCE), and the anodic and cathodic current responses are measured. As shown in Fig. 5, the voltammetric current responses for all NiO/CNTs electrodes are similar to that of pure NiO electrode. Each curve is composed of capacitive current, which originates from the phase of active materials and characteristic peaks of anodic/cathodic redox reactions which appear at ~0.28/0.05 V (vs. SCE).

Some previous reports demonstrated that NiO in an alkaline solution tends to change to $Ni(OH)_2$ at the surface [40, 41]. Therefore, above anodic/cathodic peaks are responsible for $Ni(OH)_2$/NiOOH redox reaction. Moreover, it is distinct that, in Fig. 5, the composite of NiO/CNTs=5:5 shows the largest shape area in a series of composites, indicating the highest capacitance. Such enhanced capacity proves our deduction from above section. Physical ultrasonication for CNTs creates sufficient nicks which can act as nucleation sites for $Ni(OH)_2$ nucleating, resulting in a uniform NiO coating layer on CNTs with larger specific

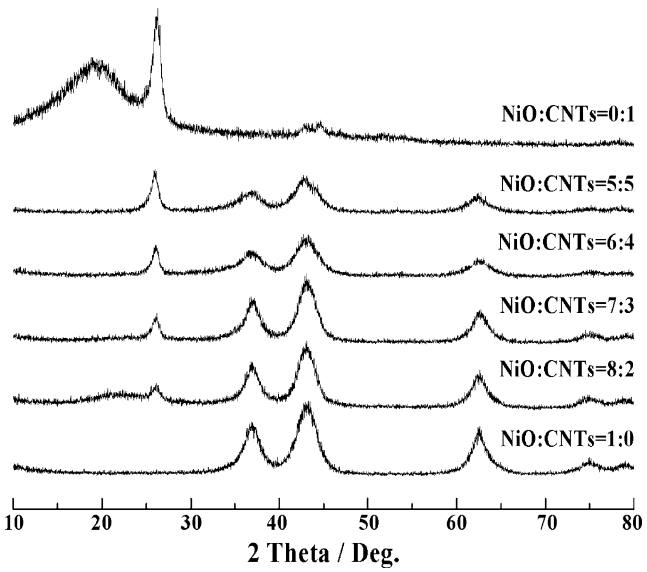

Fig. 4 XRD patterns of different mass ratios of NiO/CNTs

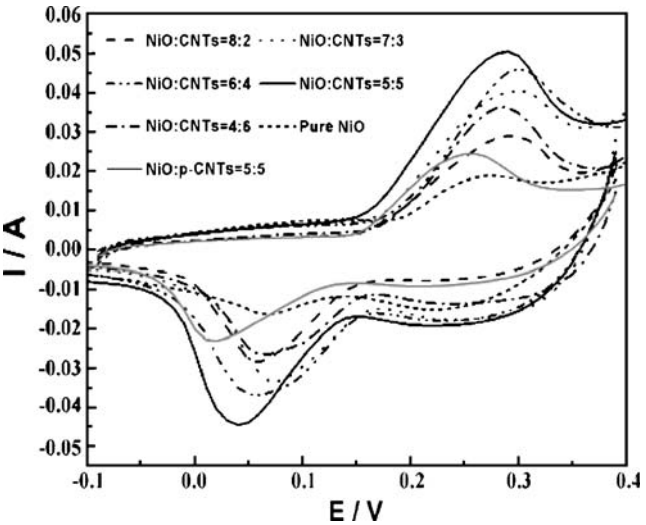

Fig. 5 Cyclic voltammograms of NiO/CNTs with different mass ratios at a scan rate of 10 mV/s in 6 M KOH electrolyte

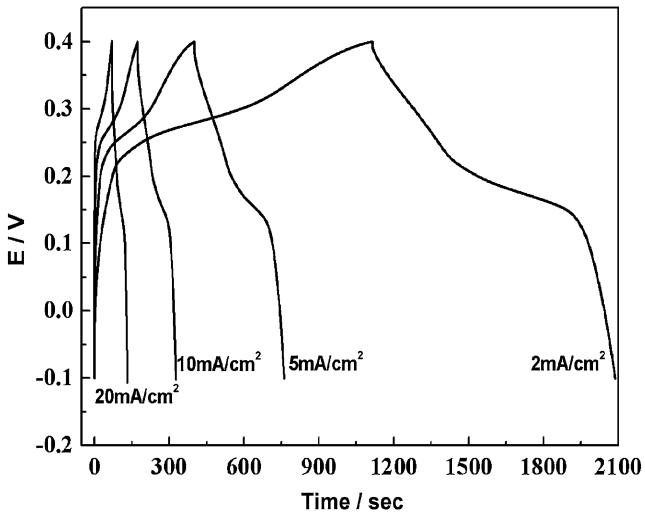

Fig. 6 The charge–discharge curves of the NiO/CNTs (NiO/CNTs= 5:5) at different current density

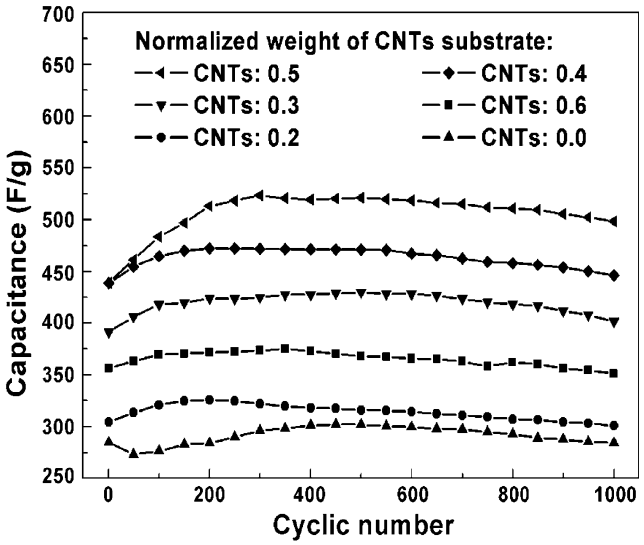

Fig. 8 Cycle-life of the different mass ratios composites at a constant current density of 5 mA/cm^2

surface area, and thus a significant increase in the charge/discharge storage capacity.

To evaluate the electrochemical capacitance of the synthesized NiO/CNTs composites, we use these materials to fabricate electrodes for ECs, and characterize with chronopotentiometric measurements. Figure 6 shows the constant current charge/discharge curve of NiO/CNTs electrodes (the mass ratio we choose is NiO/CNTs=5:5). The range of voltages for charging/discharging are from −0.1 to 0.4 V with different current density, and curves from right to left correspond to 2, 5, 10, and 20 mA/cm^2, respectively. As shown in it, the shape of the charge/discharge curve does not present the characteristic of pure double layer capacitor or amorphous ruthenium oxide capacitor, but in agreement with the CV curves. Our study in CNTs shown that its capacitance is about 30 F/g, hence here we can deduce that the capacitive behaviors of these composites are mainly attributing to pseudocapacitance of NiO matrix. So the specific capacitance of the NiO/CNTs nanotubular composites (C_m) and NiO in the composites ($C_{m'}$) are calculated as Eqs. 1 and 2, respectively:

$$C_m = \frac{C}{m} = \frac{I \times \Delta t}{\Delta V \times m} \tag{1}$$

$$C_{m'} = \frac{C}{m'} = \frac{I \times \Delta t}{\Delta V \times m \times a} \tag{2}$$

where I is the discharge current, m is the mass of the composite, ΔV the potential drop during discharging, Δt the total discharge time, and C the specific capacitance. m' is the mass of NiO in NiO/CNTs composites in one electrode and a is the weight percent of NiO in NiO/CNTs.

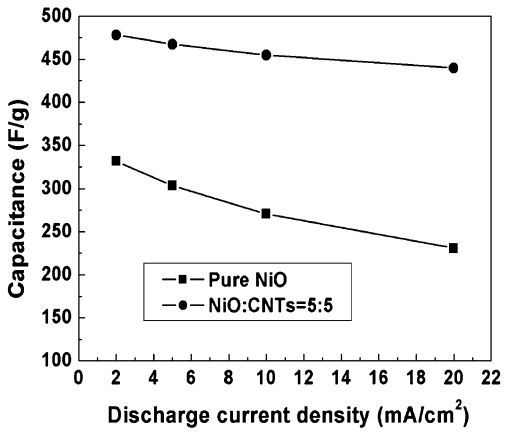

Fig. 7 Specific capacitance of pure NiO and NiO/CNTs (NiO/CNTs= 5:5) as a function of the discharge current density

Table 1 The capacitances of the NiO/CNTs composites in one electrode and the specific capacitance of the NiO in the composite were calculated from charge/discharge curves according to Equations 1 and 2, respectively

Weight percent of the NiO in NiO/CNTs composite (wt%)	Capacitance of the NiO/CNTs at 5 mA/cm^2 (F/g)	Capacitance of the NiO in composites at 5 mA/cm^2 (F/g)
100	304.70	304.70
80	326.20	405.50
70	434.05	617.07
60	472.59	781.65
50	523.37	1037.74
40	382.84	943.60

Figure 7 shows the dependence of specific capacitance on discharge current density for pure NiO and NiO/CNTs composites (NiO/CNTs=5:5). It is obvious that the specific capacitances decrease gradually with increasing discharge current density especially for pure NiO electrode. For pure NiO electrode, the specific capacitance at a discharging current density of 20 mA/cm^2 drop about 30%, compared with that at 2 mA/cm^2, while the capacitance of NiO/CNTs composite electrode drops only 10% under similar conditions. The rapid deterioration in specific capacitance for pure NiO electrode may be caused by the large internal resistance of the electrode, which leads to a large ohmic drop at high discharging current density. But for NiO/CNTs electrode, NiO matrix is coated uniformly on surface of CNTs, leading to a uniformly and highly 3D nanoporous composite and better electric conductivity; thus, it has a lower capacitance fading as discharging current density increases.

The cycle life of NiO/CNTs electrodes with different mass ratios is monitored by a chronopotentiometry measurement at 5 mA/cm^2 in 6 M KOH, as shown in Fig. 8. Meanwhile, based on Eqs. 1 and 2, the highest measured capacitance of each above electrode is also listed in the Table 1. Interestingly, all electrodes showed a slight increase in the specific capacitance, which might be due to the formation of $Ni(OH)_2$ on the surface of NiO electrode, especially at the interfacial area between NiO and alkaline solution [14, 25]. However, the pure NiO electrode shows an obvious fading subsequently, whereas NiO/CNTs electrodes reveal a stable specific capacitance during consecutive cycle test. It is noticeable that the composite, with the mass ratio of NiO/CNTs=5:5, shows the highest capacitance (523 F/g) and maintains its highest capacitance with the lowest fading. The excellent capacitive and cyclic performance is attributable to the following reasons. First, the electronic conductivity and large electrode/solution contacting interface of the composites is improved due to the presence of CNTs. Second, the nanotubular structures of NiO/CNTs composite facilitate the OH^- ion diffusion and migration during the rapid charge/discharge process.

Conclusion

In this paper, a physical ultrasonication method is employed to functionalize CNTs, which is used as a carbonaceous substrate to form NiO/CNTs composite materials. The HRTEM and SEM results show that a lot of nicks, which would favor the nucleation of the $Ni(OH)_2$, are observed on the outer surface of CNTs due to ultrasonic cavitations, and a homogeneous NiO coating layer are detected after being precipitated and calcined. Electrochemical studies demonstrate that the electrochemical performances of NiO/CNTs composites are improved greatly. The good electrochemical characteristics of NiO/CNTs composite such as maximum specific capacitance of 523 F/g and excellent cycle life can attribute to the three-dimensionally interconnected nanotubular structure with a thin film of electroactive materials.

Acknowledgments This work is supported by National Basic Research Program of China (973 Program) (No.2007CB209703), National Natural Science Foundation of China (No.20403014 and No.20633040) and Natural Science Foundation of Jiangsu Province (No.BK2006196).

References

1. Conway BE (1999) Electrochemical supercapacitors; scientific fundamentals and technological applications. Kluwer/Plenum, New York, p 13
2. Frackowiak E, Beguin F (2001) Carbon 39:937, doi:10.1016/S0008-6223(00)00183-4
3. Villers D, Jobin D, Soucy C, Cossement D, Chahine R, Breau L et al (2002) J Electrochem Soc 149:A167, doi:10.1149/1.1431575
4. Fusalba F, El Mehdi N, Breau L, Belanger D (2000) Chem Mater 12:2581, doi:10.1021/cm000011r
5. Zheng JP, Jow TR (1998) J Electrochem Soc 145:49, doi:10.1149/1.1838535
6. Liu KC, Anderson MA (1996) J Electrochem Soc 143:124, doi:10.1149/1.1836396
7. Srinivasan V, Weidner JW (1997) J Electrochem Soc 144:L210, doi:10.1149/1.1837859
8. Nam KW, Kim KB (2002) J Electrochem Soc 149:A346, doi:10.1149/1.1449951
9. Nam KW, Yoon WS, Kim KB (2002) Electrochim Acta 47:3201, doi:10.1016/S0013-4686(02)00240-2
10. Prasad KR, Miura N (2004) Appl Phys Lett 85:4199, doi:10.1063/1.1814816
11. Nam KW, Kim KB (2001) Electrochemistry 69:467
12. Lee SH, Tracy CE, Pitts JR (2004) Electrochem Solid-State Lett 7:A229
13. Zhang FB, Zhou YK, Li HL (2004) Mater Chem Phys 83:260, doi:10.1016/j.matchemphys.2003.09.046
14. Nelson PA, Owen JR (2003) J Electrochem Soc 150:A1313, doi:10.1149/1.1603247
15. Ganesh V, Lakshminarayanan V (2004) Electrochim Acta 49:3561, doi:10.1016/j.electacta.2004.03.024
16. Lin C, Ritter JA, Popov BN (1998) J Electrochem Soc 145:4097, doi:10.1149/1.1838920
17. Lee HY, Goodenough JB (1999) J Solid State Chem 144:220, doi:10.1006/jssc.1998.8128
18. Pang SC, Anderson MA, Chapman TW (2000) J Electrochem Soc 147:444, doi:10.1149/1.1393216
19. Hu CC, Tsou TW (2002) Electrochem Commun 4:105, doi:10.1016/S1388-2481(01)00285-5
20. Takasu Y, Mizutani S, Kumagai M, Sawaguchi S, Murakami Y (1999) Electrochem Solid-State Lett 2:1, doi:10.1149/1.1390714
21. Deng CZ, Pynenburg RAJ, Tsai KC (1998) J Electrochem Soc 145:L61, doi:10.1149/1.1838416
22. Wang YG, Zhang XG (2004) Electrochim Acta 49:1957, doi:10.1016/j.electacta.2003.12.023
23. Wang YG, Zhang XG (2005) J Electrochem Soc 152:671, doi:10.1149/1.1864392

24. Gao B, Zhang XG, Yuan CZ, Li J, Yu L (2006) Electrochim Acta 52:1028, doi:10.1016/j.electacta.2006.05.049
25. Nam KW, Lee ES, Kim JH, Lee YH, Kim KB (2005) J Electrochem Soc 152:A2123, doi:10.1149/1.2039647
26. Tasis D, Tagmatarchis N, Bianco A, Prato M (2006) Chem Rev 106:1105, doi:10.1021/cr050569o
27. Hirsch A, Vostrowsky O (2005) Top Curr Chem 245:193
28. Bahr JL, Tour JM (2002) J Mater Chem 12:1952, doi:10.1039/b201013p
29. Khabashesku VH, Billups WE, Margrave JL (2002) Acc Chem Res 35:1087, doi:10.1021/ar020146y
30. Niyogi S, Hamon MA, Hu H, Zhao B, Bhowmik P, Sen R et al (2002) Acc Chem Res 35:1105, doi:10.1021/ar010155r
31. Gong K, Yu P, Su L, Xiong S, Mao L (2007) J Phys Chem C 111:1882, doi:10.1021/jp0628636
32. Hudson JL, Casavant MJ, Tour JM (2004) J Am Chem Soc 126:11158, doi:10.1021/ja0467061
33. Stephenson JJ, Hudson JL, Azad S, Tour JM (2006) Chem Mater 18:374, doi:10.1021/cm052204q
34. Zhang Y, Wen Y, Liu Y, Li D, Li J (2004) Electrochem Commun 6:1180, doi:10.1016/j.elecom.2004.09.016
35. Neppiras EA (1980) Phys Rep 61:159, doi:10.1016/0370-1573(80)90115-5
36. Didenko YT, McNamara WB, Suslick KS (1999) J Am Chem Soc 121:5817, doi:10.1021/ja9844635
37. McNamara WB, Didenko YT, Suslick KS (1999) Nature 401:772, doi:10.1038/44536
38. Xing W, Li F, Yan ZF, Lu GQ (2004) J Power Sources 134:324, doi:10.1016/j.jpowsour.2004.03.038
39. Kim HJ, Jeon KK, Heo JG, Lee JY, Kim C, An KH et al (2003) Adv Mater 15:1757, doi:10.1002/adma.200304942
40. Pourbaix M (1974) Atlas of electrochemical equilibria in aqueous solutions. NACE, Houston
41. Bouessay I, Rougier A, Tarascon M (2004) J Electrochem Soc 151:H145, doi:10.1149/1.1731584